Intrinsic optical signals in neural tissues: measurements, mechanisms, and applications

Christopher Fang-Yen and Michael S. Feld

G. R. Harrison Spectroscopy Laboratory, Massachusetts Institute of Technology, Cambridge, MA 02139

Signaling phenomena in nerve tissues are accompanied by a number of intrinsic optical signals, including changes in absorption, scattering, birefringence, refractive index, and nerve geometry. We review these signals, various techniques for their measurement, possible mechanisms for their origin, and discuss their present and potential applications in functional neural imaging.

Introduction

In 1949 Hille and Keynes (*1*) demonstrated that electrical stimulation modulates the light-scattering properties of an excised crab leg nerve. The nerve's opacity exhibited a transient change of about 1 part in 10^5 during the action potential. These initial studies were followed by reports of changes in scattering, birefringence (*2*), and optical activity (*3*) during the action potential in numerous invertebrate and vertebrate nerve preparations, including lobster leg nerve (*4*), squid fin nerve (*4*), squid giant axon (*2, 5, 6*), rabbit vagus nerve (*7*), pike olfactory nerve (*7*), and garfish olfactory nerve (*8*). The measurement of such intrinsic changes in almost every nerve preparation tested suggested that the optical effects could be used to monitor neuronal activity without invasive

From *New Approaches in Biomedical Spectroscopy*, edited by K. Kneipp, R. Aroca, H. Kneipp, and E. Wentrup-Byrne, Oxford University Press (2007)

electrophysiological probes or contrast agents (*9*). More recently, the repertoire of optical phenomena has expanded to include scattering and refractive index changes in dissociated neuron cultures (*10, 11*), fast and slow scattering changes in brain slices (*12*), and scattering in intact brain (*13*). Activity-dependent optical changes are often called intrinsic optical signals, to distinguish them from *extrinsic* optical effects such as fluorescence changes of externally applied dyes.

In parallel with optical recordings, researchers have also observed small, rapid mechanical motions in nerves during the action potential, initially in crab nerve bundles (*14-16*). Motions are typically on the order of 1 nanometer and correspond to a "swelling", i.e. a transient increase in diameter. The mechanical and optical phenomena are likely to be related, since scattering properties depend sensitively on scatterer geometry.

Optical studies of the intact brain surface have revealed a different type of intrinsic optical signal: near-infrared absorption changes caused by changes in local blood volume and/or oxygenation. Activity-dependent modulation of brain reflectance by ~0.5% has been observed (*17*) and attributed primarily due to the neurovascular response. Similar hemodynamic changes in relatively deep brain tissue have been measured transcranially using diffuse optical tomography (*18*).

Interest in intrinsic optical signals has generally concerned their potential applications as functional neural imaging techniques. Of the intrinsic optical signals reviewed here, only the imaging of slow changes in brain surface reflectance has so far become firmly established as such a technique, having been used very successfully in studies of functional architecture of the mammalian cortex (*19*). In fact, the term "intrinsic optical signals" is often used to refer specifically to near-infrared imaging of hemodynamic changes on the brain surface. What then are the prospects for application of the "other" intrinsic signals: the birefringence, scattering, and refractive index changes, and mechanical motions?

In this paper we review the various types of intrinsic optical signals and the technologies for measuring them, with emphasis on non-hemodynamic signals. We discuss interpretations and proposed mechanisms for the intrinsic signals and evaluate the status of efforts to use them as a basis for functional neuroimaging techniques.

Intrinsic signals in nerves and cultured neurons

Initial studies

Early experiments for measuring scattering and birefringence changes (*1, 2, 5, 6*) used variations on a simple experimental setup. A nerve was dissected from a specimen and placed in a nerve chamber containing a physiological bath solution and stimulation and recording electrodes. Extracellular or intracellular electrodes were used for nerve bundle and giant axon experiments, respectively. Light from an incandescent lamp was focused onto the nerve and scattered light imaged onto a photodiode or photomultiplier tube. Most experiments considered the angular dependence of scattered light, typically via measurements in the near-forward (0 degree) and near-right angle (90 degree) directions, via a movable detector assembly. Photodetector outputs were amplified and averaged by a signal averager. Several thousand traces were averaged to obtain a reasonable signal to noise ratio.

Typical data from nerve bundles (e.g. Figure 1 from Tasaki *et al* (*4*)) generally showed a fast $\sim 10^{-5}$ relative increase in scattering at 45-90 degrees during the action potential, followed by an *decrease* in scattering over longer time scales (*4*). Results from single axons of squid were roughly an order of magnitude smaller (*2*). Considerable variability (over a factor ~10) in responses between specimens of the same type was found.

For birefringence measurements, the sample was placed between crossed polarizers and scattering measured in the forward direction. Largest effects were observed with the axis of the nerve bundle oriented 45 degrees from the direction of either polarizer (*2*). Transmitted intensity changes varied from $\sim 10^{-6}$ to $\sim 10^{-4}$, with a sign corresponding to an increase in birefringence (*4*). Nerves exhibit an activity-independent intrinsic birefringence due to longitudinally aligned microtubules in axoplasm and may also have significant form birefringence.

Several explanations were suggested to account for the activity-dependent modulation of scattering and birefringence. Scattering changes may result from transient increases in diameter or changes in ionic composition near the axon membrane (*8*). Birefringence changes could be caused by polarization and alignment of axon membrane protein molecules due to changes in membrane potential (*1, 2, 10*). Although the membrane is only a few nanometers thick, order-of-magnitude estimates for polar molecules suggest that such an electro-optic mechanism would be sufficiently large to account for the birefringence observations. Another explanation for birefringence changes involves the mechanical compression of the membrane due to membrane charge

(electrostriction effect) (*2*). These mechanisms will be revisited in the discussion of other intrinsic optical experiments.

Scattering in cultured neurons

A study by Stepnoski *et al* (*10*) of scattering changes in cultured neurons from *Aplysia californica* (a marine invertebrate) represents the most detailed attempt so far to interpret intrinsic optical changes in terms of a specific biophysical model.

Cultured neurons containing an extensive array of processes (nerve fibers) were placed in a microscope illuminated with a darkfield configuration such that only light which scatters by 3 degrees or more is detected. Scattered light intensity from a field of view containing many processes was found to be modulated nearly linearly with changes in membrane potential (Figure 2), with a proportionality constant on the order of 10^{-5} relative scattering change per mV. Changes were large enough to be detected without signal averaging. Individual action potentials could be resolved in a spike train induced by injecting a constant level current pulse into the cell body.

To further investigate the intrinsic changes, the authors performed angle-resolved light scattering measurements. A 633 nm laser was focused onto single axons and the scattering intensity and voltage-dependence of scattering were measured for as a function of azimuthal scattering angle. The baseline scattering pattern fell off from 0 degrees in a series of peaks and troughs, as expected from scattering from a cylindrically symmetric dielectric. The change in scattering during a voltage spike was observed to alternate in sign as a function of angle. The magnitude of small-angle scattering was shown to be in agreement with the darkfield scattering results.

To explain the angular dependence results quantitatively, the authors developed a model based on dipoles in the axon membrane with voltage-dependent reorientation in the transmembrane field. The dipole polarization leads to a difference in refractive index between light polarized normal and tangential to the membrane. A linear change in refractive index with voltage was assumed; this is the linear electro-optic or Pockels effect. This model based on dipole reorientation produced a reasonably good agreement with experimental data. By contrast, the data excluded models based on (i) an isotropic change in membrane index, (ii) modulation of radial refractive index only, and (iii) voltage-dependent modulation of the bulk refractive index in the axon. Surprisingly, the authors do not discuss the possibility that scattering changes may be due at least in part to transient diameter changes in the axons, observations of which are discussed later in this review.

Voltage-induced refractive index shifts will lead to shifts in optical path length (OPL) of transmitted light; in a related study, Laporta and Kleinfeld (*11*) use a Mach-Zehnder laser interferometer resembling a differential interference contrast (DIC) microscope to probe OPL shifts through a few axons of a lobster leg nerve during the action potential. With an averaging of 100 trials, a peak OPL change of about 0.3 angstroms was observed. Recently, efforts to measure similar signals in single cultured neurons using interferometric quantitative phase microscopy techniques have been reported (*20*).

Nerve changes measured with Optical Coherence Tomography

Optical Coherence Tomography (OCT) (*21*) is a relatively new imaging technique in which a probe beam of broadband light is scanned across a sample and the backscattered light is mixed with a reference field to create depth-resolved, 2D or 3D scattering profiles in biological tissues. OCT can be thought of as an optical analogue of ultrasound imaging, with 2-5 micron spatial resolution and 1-2 mm penetration depths. Although it is primarily known for applications in retinal, skin, and intravascular imaging (*22*), recently OCT has begun to be applied to measurements of intrinsic signals in nerve tissues (*23*). The depth gating property of OCT allows imaging scattering changes in three dimensions and helps to reject the multiply-scattered light contributions in reflectance imaging.

Maheswari *et al* (*24*) used OCT to measure slow intrinsic scattering signals in exposed cat visual cortex during horizontal and vertical grating stimuli. In order to take advantage of OCT's coherence gating properties, the authors focused on depth-dependent rather than lateral-dependent changes in reflectance, and found preliminary evidence that the modular organization of visual cortex also extends in the depth direction. Lazebnik *et al* (*25*) measured scattering changes in dissociated *Aplysia* nerve fibers in vitro and demonstrated localized reversible scattering increases when electrical stimulation was applied.

Two recent OCT studies measured slow scattering changes in the dissociated vertebrate retina, in which intrinsic signals had been measured by other techniques (*26*). In one study, functional changes from light-activated frog retina in vitro (*27*) were recorded. In another, increases in scattering at particular depths were reported in rabbit retina (*28*).

Mechanical displacements: optical and non-optical approaches

Observations of nerve mechanical motions during the action potential have been performed with various contact and combined contact/optical techniques,

including piezoelectric sensors (*29*), volume change measurements (*30*), measurements of scattering of attached beads (*15*) and optical lever recordings (*31*).

Optical interferometry is capable of measuring changes many orders of magnitude smaller than the wavelength of light, and is well-suited for measuring nanometer-scale changes in nerve tissues. Applications of optical interferometry to measure motions in excitable tissues were described in Sandlin *et al* (*32*) and Hill *et al* (*33*), who measured a 1.8 nm, ~1 ms contraction displacement followed by a slow swelling in a crayfish giant axon coated with gold particles to increase reflectivity. Recently two optical interferometric techniques (*34, 35*) been developed for measuring action potential-induced displacements in nerves without scattering contrast agents to the tissues. Two keys to these approaches have been the use of low coherence (broadband) light to achieve depth-selective measurements, and phase-referencing (*36*), in which the phase of light reflected from a sample is measured relative to a fixed reference reflection, to reduce interferometer noise.

In Akkin *et al*, a polarization-sensitive low coherence fiber interferometer was used to measure ~0.5 nm, 1 ms displacements in crayfish leg nerves. Calcite prisms are used to compensate for optical path delay between the nerve reflection and a reference cover glass. The authors suggested that the technology may allow noninvasive detection of various neuropathies.

Fang-Yen *et al* used a heterodyne dual-beam low coherence interferometer to measure displacements in a lobster leg nerve (Figure 3). A free space Michelson interferometer containing acousto-optic modulators was used to compensate for the path length difference between sample and reference surfaces. An upward displacement of the upper nerve surface of ~5 nm was measured without signal averaging. The threshold and saturation stimulus current amplitudes for the optical and electrical signals were shown to be nearly identical, strongly suggesting that displacements were directly related to the action potentials.

Initial explanations for the surface displacements were concerned with hydration due to imbalances of sodium and potassium ions involved in the generation of the action potential (*37*). However, estimates of the scale of such an effect give swelling magnitudes at least 2 orders of magnitude smaller than observed (*38*). It was suggested that intrinsic motions may arise from a gel phase transition in axoplasm due to a sodium/calcium ion binding exchange (*38*), but direct evidence for this model has not yet been found.

More recently, it has been suggested that voltage-dependent motions may arise from a fundamental electromechanical coupling between membrane potential and membrane mechanical properties. A study combining patch clamp electrophysiology and atomic force microscopy (AFM) measured voltage-dependent modulations in membrane potential (*39*). A theoretical study (*40*) considered the effect of two electrostatic properties of dielectrics,

electrostriction and piezoelectricity, on the nerve membrane to predict changes in axon dimensions during the action potential.

Intrinsic signals in brain slices

The recording of optical changes in brain tissue slices was pioneered by Lipton (*12*), who used a photodiode to measure reflectance at 176 degrees from the surface of hippocampal slices submerged in a bath medium. Electrical stimulation led to decrease in scattering, which was attributed to cell swelling. The association between transparency and cell swelling had been established on the basis of experiments with cell suspensions (*41*), and protein solutions (*42*).

Current experiments use near-infrared illumination and a charged-coupled device (CCD) camera to image the slice in reflection mode, transmission mode, or both. Scattering changes may be very large, more than 20% over several minutes, and may be readily observed using relatively simple sources and detectors.

A great deal of the literature on optical changes in brain slices concerns the phenomenon of spreading depression (SD) (*43*), a self-propagating wave of depolarization associated with depression of neuronal activity for several minutes, dramatic changes in extracellular and intracellular ionic concentrations, and cellular swelling. SD is implicated in a number of pathological conditions, although its mechanisms and significance remain unclear. Optically, SD generally creates an increase in hippocampal slice reflectance despite the cell swelling effect, although this depends on the conditions of the experiments and the method of SD induction (*44*). One study (*45*) attempts to clarify the picture by suggesting that at least two different mechanisms underlie intrinsic signals in hippocampal slices. First, light scattering decreases due to cell swelling and increase of interstitial volume. Second, during SD and strong hypotonic conditions with severely decreased interstitial volume, light scattering increases due to swelling of cellular organelles, especially mitochondria.

MacVicar and Hochman (*46*) examined intrinsic optical changes in hippocampal slices induced by synaptic transmission. Based on results from perturbing extracellular ionic concentrations and administering various ion transport inhibitors, the authors suggested that intrinsic signals may arise from glial swelling due to potassium released by neurons during excitation.

Although most brain slice studies have measured slow (~1 sec) optical changes, optical changes on time scales comparable to the electrical signals have been reported in some preparations.

Large and rapid changes in light scattering was seen in nerve terminals of the mouse neurohypophysis, the posterior lobe of the pituitary gland (*47*). By detecting transmitted light of a 600-850 nm source through a microscope, large

~0.3% intrinsic peaks were observed, without averaging, and with time course similar to the action potential. The origin of the transient decreases in light scattering (increases in transmission) was unclear. Suggestions included loss of scattering from secretory vesicles during exocytosis, changes in contents of secretory vesicles, or structural changes associated with rapid changes in calcium concentrations.

Intrinsic signals in the intact brain

Brain surface imaging

Functional imaging of the exposed and intact brain surface, the most well-known type of intrinsic signal imaging, was developed by Grinvald and colleagues (*19, 48, 49*). The brain surface is illuminated with light at one or multiple wavelengths, and reflectance images are captured with a CCD camera during stimulus presentation (e.g. Figure 4). Since typical activity-dependent changes in reflectivity are in the range 0.1% – 0.5%, reflectance images are typically measured relative to a baseline "blank" image.

Intrinsic signals in the brain are much more complex than nerve or brain slice preparations, in part due to vascular responses to neural activity. Brain reflectance is modulated by at least three factors: (i) chromophore oxidation states, notably of hemoglobin and cytochrome oxidase, (ii) changes in blood volume, and (iii) light scattering changes (*50*). Metabolic demands associated with neuronal activity create a local depletion in hemoglobin oxygenation in microcapillaries, which increases tissue absorption at wavelengths 600-650 nm. The vascular system responds to this change by increasing blood flow to the region, leading to a net *increase* in oxy-hemoglobin within 1-2 seconds. The vascular response is less well-localized than the original oxygen depletion response. Similar dynamics including an "initial dip" in oxygenation have been reported in fMRI (*51*). Scattering changes are thought to be similar in nature to those observed in brain slices.

Different components in the brain reflectance images can be distinguished by their different time courses and wavelength dependence. Wavelength-selective optical filters can be used to emphasize different signal components. At 605 nm, the oxymetry component is dominant; at 630 nm blood volume and hemoglobin saturation; at wavelengths greater than 700 nm absorption changes are small and the scattering signal dominates (*50*).

Intrinsic imaging has become an important tool for studying functional cortical maps – the spatial patterning of activation during a certain type of

stimulus or behavior – in visual cortex, motor cortex, somatosensory cortex, olfactory bulb, and auditory cortex. For a detailed review of this large field see (*52*). A particular advantage of optical imaging, compared with techniques such as electrode recording and radiolabel tracing, is the ability to record multiple maps in succession in the same subject. This has led to important findings about relationships between different cortical columnar systems (*53-55*).

Intrinsic signal imaging of the brain surface has been applied to humans intra-operatively. One area of study concerns the mapping of functional boundaries to minimize damage during operations to remove tumors, epileptic foci, or other tissues (*56-58*). Studies have delineated human somatosensory maps (*58*) and areas involved in language (*57*).

While most brain surface imaging studies are concerned with slow absorption and scattering changes, a few measurements of fast scattering changes have been reported. Rector *et al* (*59*) used a deep-brain fiber optic illuminator and fiber imaging system to record ~0.1% stimulus-dependent light scattering changes in cat dorsal hippocampus. Light scattering peaked about 20 ms after stimulation and coincided with neuronal population spiking. A longer-lasting scattering component peaked 100-500 ms post-stimulus, probably reflecting postsynaptic potentials. Recordings of similar changes in rat brain stem (*13*) and whisker barrel cortex (*60*) have also been reported.

Transcranial measurements: diffuse optical methods

For intrinsic optical effects in the human brain to be detected noninvasively, light must pass through the skin and skull, interact with the brain, then pass again through skull and skin to detectors (*61*). In diffuse optical imaging, an array of light sources (typically light emitting diodes) and an array of photodetectors are arranged on the head. Sources used are typically in the wavelength range 650nm-1000nm, at which tissue absorption is negligible compared to scattering. The density of photons in tissue is considered to obey a diffusion equation with absorption (*62*). Two wavelengths are often used to perform spectroscopy of the oxygenation states.

Three types of diffuse optical imaging have been developed: (i) time domain imaging, (ii) frequency domain image, and (iii) continuous-wave imaging. In time domain imaging, extremely short (~ps) pulses of light are introduced into the head and the temporal distribution of photons measured by the detectors gives information about absorption and scattering in the brain. Frequency domain techniques use sources with high frequency (~10-100 MHz or more) modulation in amplitude; detectors record amplitude and phase shift of the field. Continuous-wave systems use unmodulated or slowly modulated sources and measure only the intensity of the returning light. (*18*). As in brain

surface imaging, diffuse imaging signals are primarily dominated by absorptive hemodynamic changes.

Imaging of intrinsic changes by diffuse techniques is performed via inversion algorithms (*61*). Because of the strong scattering, spatial resolution is typically limited to several centimeters, and penetration depths to about 3 cm.

Diffuse optical imaging has been used to investigate cerebral responses to visual, auditory, and other sensory stimuli, motor activity, and language, among others. Although diffuse imaging has a lower spatial resolution than fMRI and cannot generally used to probe deep brain regions, diffuse optical imaging technology has the advantage of being portable, relatively inexpensive, and can be applied for the study of states and behaviors incompatible with MRI imaging.

Several authors have reported fast scattering measurements in transcranial diffuse optical experiments (*63, 64*), although the robustness of these measurements has been questioned (*65*).

Discussion and conclusions

The wide range of intrinsic effects reviewed here can be seen as falling into two classes. On one hand are the absorption-based changes, primarily caused by blood oxygenation and flow changes in response to neural activity. These effects are slow and have modest spatial resolution which can resolve cortical columns but not single neurons. However, they arise from relatively robust mechanisms and are closely correlated with other measures of activity. As such, brain surface reflectance imaging is widely used to measure spatial distributions of cortical activity, and applications of noninvasive diffuse optical techniques are growing steadily. On the other hand are the non-hemodynamic phenomena such as scattering, birefringence, and mechanical changes, which can have time resolution comparable to the underlying electrical signals, and spatial resolution to the level of single nerve fibers. However, they are generally difficult to measure and interpret, and their mechanisms are relatively poorly understood. As a result, applications of these measurements remain quite limited.

What will be required to develop these non-hemodynamic measurements into useful functional neuroimaging tools? Three related components are needed: (i) continued development of optical techniques for measuring these signals robustly and with high sensitivity, (ii) improved understanding of the mechanisms underlying intrinsic signals, and (iii) a clear interpretation of the measurements, which may involve elucidating and separating contributions from different processes.

Where will measurement of non-hemodynamic intrinsic changes first have important applications? We suggest that in the near future the most likely useful role will be for imaging activity in cultured neurons and neural networks (*10,*

66). Cultured neurons are widely used to study nervous systems at the molecular, cellular, and synaptic levels. Collections of connected neurons are emerging as a model system for biological neural circuits; such networks have been shown to exhibit basic forms of network plasticity (*67*). In these relatively simple, controlled preparations, very small optical changes can be measured without artifacts from animal motions or cross-talk from large numbers of neurons. Interpretations of the intrinsic signals may be easier due to a reduced complexity of the overall system. Manipulations of the preparations can be more readily performed, for investigation of signal mechanisms or optimization of conditions for signal measurement. As a technique for monitoring signaling in many neurons simultaneously, a fast intrinsic optical method would offer better spatial localization compared with multi-electrode array (MEA) techniques (*68*), and avoid phototoxicity and photobleaching problems of calcium-sensitive and voltage-sensitive fluorescent dye imaging (*69*).

In summary, nerve tissues display a wide variety of intrinsic optical phenomena, most of which are not yet well understood. Intrinsic signals which are hemodynamic in origin are now being commonly applied in functional imaging. Others such as fast scattering and nerve geometry changes have made inroads more slowly, due to challenges in measuring, understanding, and interpreting the signals. Novel optical imaging techniques have the potential to overcome these challenges, particularly in studies with cultured neurons.

References

1. Hill, D.; Keynes, R. *J Physiol* **1949,** *108*, 278-281.
2. Cohen, L. B.; Keynes, R. D.; Hille, B. *Nature* **1968,** *218*, 438-441.
3. Watanabe, A. *J Physiol* **1987,** *389*, 223-53.
4. Tasaki, I.; Watanabe, A.; Sandlin, R.; Carnay, L. *Proc Natl Acad Sci U S A* **1968,** *61*, 883-8.
5. Cohen, L. B.; Keynes, R. D.; Landowne, D. *J Physiol* **1972,** *224*, 701-25.
6. Cohen, L. B.; Keynes, R. D.; Landowne, D. *J Physiol* **1972,** *224*, 727-52.
7. von Muralt, A. *Philos Trans R Soc Lond B Biol Sci* **1975,** *270*, 411-23.
8. Tasaki, I.; Byrne, P. M. *Jpn J Physiol* **1993,** *43 Suppl 1*, S67-75.
9. Cohen, L. *Annual Review of Physiology* **1989,** *51*, 487-490.
10. Stepnoski, R. A.; Laporta, A.; Raccuia-Behling, F.; Blonder, G. E.; Slusher, R. E.; Kleinfeld, D. *Proceedings of the National Academy of Sciences of the United States of America* **1991,** *88*, 9382-9386.
11. Laporta, A.; Kleinfeld, D. *Interferometric detection of action potentials in vitro*; Imaging in Neuroscience and Development: A Laboratory Manual Cold Spring Harbor Laboratory Press: New York, 2005, pp 539-543.

12. Lipton, P. *J Physiol* **1973,** *231*, 365-83.
13. Rector, D. M.; Rogers, R. F.; Schwaber, J. S.; Harper, R. M.; George, J. S. *Neuroimage* **2001,** *14*, 977-94.
14. Iwasa, K.; Tasaki, I.; Gibbons, R. C. *Science* **1980,** *210*, 338-9.
15. Iwasa, K.; Tasaki, I. *Biochem Biophys Res Commun* **1980,** *95*, 1328-31.
16. Tasaki, I.; Iwasa, K.; Gibbons, R. C. *Jpn J Physiol* **1980,** *30*, 897-905.
17. Grinvald, A.; Lieke, E.; Frostig, R. D.; Gilbert, C. D.; Wiesel, T. N. *Nature* **1986,** *324*, 361-364.
18. Villringer, A.; Chance, B. *Trends Neurosci* **1997,** *20*, 435-42.
19. Boenhoffer, T.; A., G. *Optical imaging based on intrinsic signals. The methodology.*; Brain Mapping: the methods; Academic Press: London, 1996; Vol. pp 55-97.
20. Fang-Yen, C.; Oh, S.; Song, S.; Seung, H. S.; Dasari, R. R.; Feld, M. S., Differential Heterodyne Mach-Zehnder Interferometer for Measurement of Nanometer-Scale Motions in Living Cells. In *Optical Society of America Topical Meeting in Biomedical Optics*, Optical Society of America: Ft. Lauderdale, FL, 2006
21. Huang, D.; Swanson, E. A.; Lin, C. P.; Schuman, J. S.; Stinson, W. G.; Chang, W.; Hee, M. R.; Flotte, T.; Gregory, K.; Puliafito, C. A.; Fujimoto, J. G. *Science* **1991,** *254*, 1178-1181.
22. Fercher, A. F.; Drexler, W.; Hitzenberger, C. K.; Lasser, T. *Reports on Progress in Physics* **2003,** *66*, 239-303.
23. Boppart, S. A. *Psychophysiology* **2003,** *40*, 529-41.
24. Maheswari, R. U.; Takaoka, H.; Kadono, H.; Homma, R.; Tanifuji, M. *J Neurosci Methods* **2003,** *124*, 83-92.
25. Lazebnik, M.; Marks, D. L.; Potgieter, K.; Gillette, R.; Boppart, S. A. *Opt Lett* **2003,** *28*, 1218-20.
26. Harary, H. H.; Brown, J. E.; Pinto, L. H. *Science* **1978,** *202*, 1083-5.
27. Yao, X. C.; Yamauchi, A.; Perry, B.; George, J. S. *Appl Opt* **2005,** *44*, 2019-23.
28. Bizheva, K.; Pflug, R.; Hermann, B.; Povazay, B.; Sattmann, H.; Qiu, P.; Anger, E.; Reitsamer, H.; Popov, S.; Taylor, J. R.; Unterhuber, A.; Ahnelt, P.; Drexler, W. *Proc Natl Acad Sci U S A* **2006,** *103*, 5066-71.
29. Tasaki, I.; Kusano, K.; Byrne, P. M. *Biophys J* **1989,** *55*, 1033-40.
30. Tasaki, I.; Byrne, P. M. *Biophys J* **1990,** *57*, 633-5.
31. Yao, X. C.; Rector, D. M.; George, J. S. *Appl Opt* **2003,** *42*, 2972-8.
32. Sandlin, R.; Lerman, L.; Barry, W.; Tasaki, I. *Nature* **1968,** *217*, 575-6.
33. Hill, B. C.; Schubert, E. D.; Nokes, M. A.; Michelson, R. P. *Science* **1977,** *196*, 426-8.
34. Akkin, T.; Davé, D.; Milner, T.; Rylander, H. *Opt. Express* **2004,** *12*, 2377-2386.

35. Fang-Yen, C.; Chu, M. C.; Seung, H. S.; Dasari, R. R.; Feld, M. S. *Opt Lett* **2004,** *29*, 2028-30.
36. Yang, C.; Wax, A.; Hahn, M. S.; Badizadegan, K.; Dasari, R. R.; Feld, M. S. *Optics Letters* **2001,** *26*, 1271-1273.
37. Hill, D. K. *J Physiol* **1950,** *11*, 304-27.
38. Tasaki, I. *Physiol Chem Phys Med NMR* **1988,** *20*, 251-68.
39. Zhang, P. C.; Keleshian, A. M.; Sachs, F. *Nature* **2001,** *413*, 428-32.
40. Gross, D.; Williams, W. S.; Connor, J. A. *Cell Mol Neurobiol* **1983,** *3*, 89-111.
41. Shapiro, H.; Parpart, A. *J Cell Comp Physiol* **1937,** *10*, 147-163.
42. Barer, R.; Ross, K. F.; Tkaczyk, S. *Nature* **1953,** *171*, 720-4.
43. Leão, A. *J Neurophysiol* **1944,** *7*, 359-390.
44. Aitken, P. G.; Fayuk, D.; Somjen, G. G.; Turner, D. A. *Methods* **1999,** *18*, 91-103.
45. Fayuk, D.; Aitken, P. G.; Somjen, G. G.; Turner, D. A. *J Neurophysiol* **2002,** *87*, 1924-37.
46. MacVicar, B. A.; Hochman, D. *J Neurosci* **1991,** *11*, 1458-69.
47. Salzberg, B. M.; Obaid, A. L.; Gainer, H. *J Gen Physiol* **1985,** *86*, 395-411.
48. Frostig, R. D.; Lieke, E. E.; Ts'o, D. Y.; Grinvald, A. *Proc Natl Acad Sci U S A* **1990,** *87*, 6082-6.
49. Grinvald, A.; Frostig, R. D.; Siegel, R. M.; Bartfeld, E. *Proc Natl Acad Sci U S A* **1991,** *88*, 11559-63.
50. Zepeda, A.; Arias, C.; Sengpiel, F. *J Neurosci Methods* **2004,** *136*, 1-21.
51. Kim, D. S.; Duong, T. Q.; Kim, S. G. *Nat Neurosci* **2000,** *3*, 164-9.
52. Pouratian, N.; Sheth, S. A.; Martin, N. A.; Toga, A. W. *Trends Neurosci* **2003,** *26*, 277-82.
53. Bartfeld, E.; Grinvald, A. *Proc Natl Acad Sci U S A* **1992,** *89*, 11905-9.
54. Bosking, W. H.; Crowley, J. C.; Fitzpatrick, D. *Nat Neurosci* **2002,** *5*, 874-82.
55. Hubener, M.; Shoham, D.; Grinvald, A.; Bonhoeffer, T. *J Neurosci* **1997,** *17*, 9270-84.
56. Cannestra, A. F.; Black, K. L.; Martin, N. A.; Cloughesy, T.; Burton, J. S.; Rubinstein, E.; Woods, R. P.; Toga, A. W. *Neuroreport* **1998,** *9*, 2557-63.
57. Haglund, M. M.; Ojemann, G. A.; Hochman, D. W. *Nature* **1992,** *358*, 668-71.
58. Toga, A. W.; Cannestra, A. F.; Black, K. L. *Cereb Cortex* **1995,** *5*, 561-5.
59. Rector, D. M.; Poe, G. R.; Kristensen, M. P.; Harper, R. M. *J Neurophysiol* **1997,** *78*, 1707-13.
60. Rector, D. M.; Carter, K. M.; Volegov, P. L.; George, J. S. *Neuroimage* **2005,** *26*, 619-627.
61. Strangman, G.; Boas, D. A.; Sutton, J. P. *Biol Psychiatry* **2002,** *52*, 679-93.

62. Boas, D. A.; Dale, A. M.; Franceschini, M. A. *Neuroimage* **2004,** *23 Suppl 1*, S275-88.
63. Gratton, G.; Corballis, P. M. *Psychophysiology* **1995,** *32*, 292-9.
64. Franceschini, M. A.; Boas, D. A. *Neuroimage* **2004,** *21*, 372-86.
65. Steinbrink, J.; Kempf, F. C.; Villringer, A.; Obrig, H. *Neuroimage* **2005,** *26*, 996-1008.
66. Banker, G.; Goslin, K. *Culturing Nerve Cells*; MIT Press: Cambridge, 1998
67. Bi, G.; Poo, M. *Nature* **1999,** *401*, 792-6.
68. Novak, J. L.; Wheeler, B. C. *J Neurosci Methods* **1988,** *23*, 149-59.
69. Jin, W.; Zhang, R. J.; Wu, J. Y. *J Neurosci Methods* **2002,** *115*, 13-27.

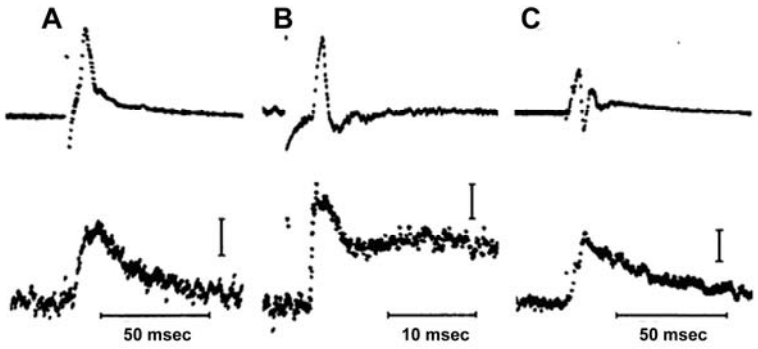

Figure 1. Top: electrophysiological recordings of action potentials of (a) spider crab nerve, (B) squid fin nerve, (C) lobster nerve. Bottom: associated changes in light scattering at 90 degrees. Vertical bars: 10^{-5}, 2×10^{-5}, and 3×10^{-5} relative increases in light intensity for A, B, and C, respectively. From Tasaki et al (4).

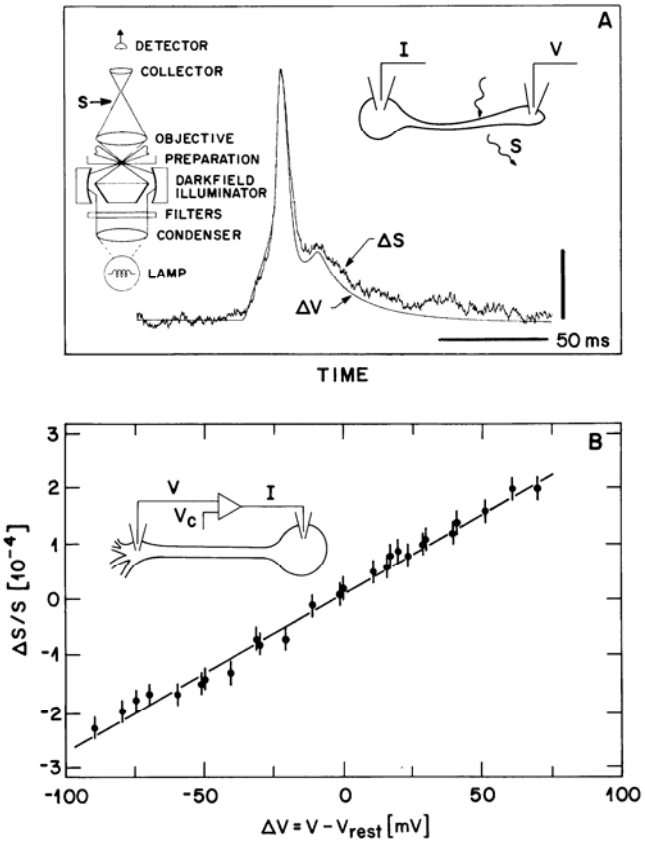

Figure 2. (A) Simultaneous optical and intracellular recordings from Aplysia neuron. ΔS: scattering change; ΔV: voltage change. Inset: schematic of darkfield light scattering setup. (B) Demonstration of linear relationship between scattered change and potential change. From Stepnoski et al (10).Copyright (c) 1991 National Academy of Sciences.

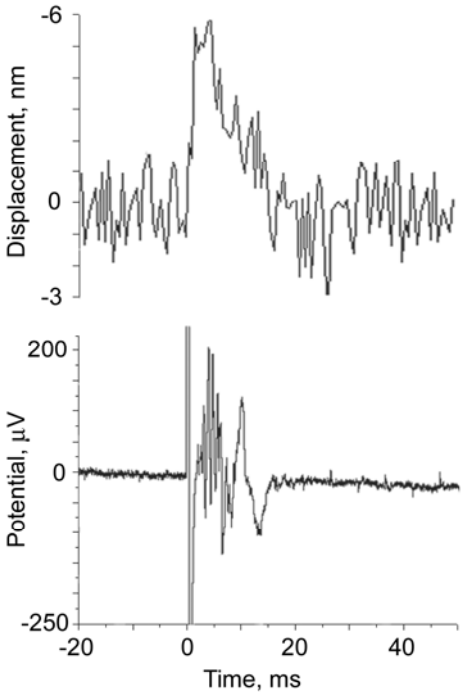

Figure 3. Single-shot interferometric measurement of rapid displacements in a lobster leg nerve during the action potential. Top, displacement signal; bottom: simultaneous recording from extracellular electrodes showing compound action potential. Spike at t=0 is stimulus artifact From Fang-Yen et al (35). Copyright (c) 2004 Optical Society of America.

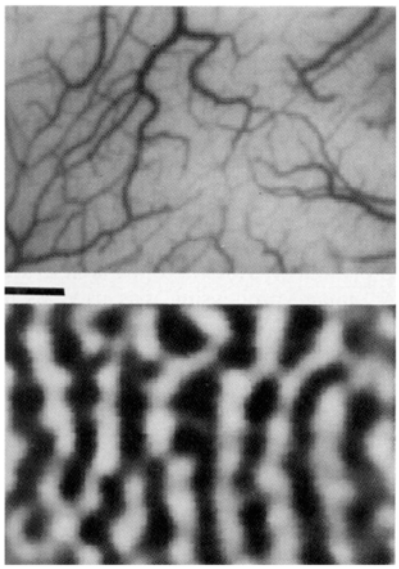

Figure 4. Imaging of ocular dominance columns in monkey visual cortex obtained by monocular presentation of a video movie. Top: vasculature of imaged area, illuminated with green light. Bottom: Ocular dominance map obtained by dividing average of 48 cortical images during right eye stimulus with average of 48 cortical images during left eye stimulus. Scale bar = 1 mm. From Grinvald et al (49). Copyright (c) 1991 National Academy of Sciences.